A New Technique for Processing GLONASS Carrier Phase Measurements over Medium Length Baselines using IGS Products

Nguyen, Lau N.,[1] Ha, Hoa M.,[2] and Coleman, R.[3]
[1]Department of Geomatics Engineering, Ho Chi Minh City University of Technology, Vietnam
[2]Vietnam Institute Geodesy and Cartography, Vietnam
[3]Institute for Marine and Antarctic Studies, University of Tasmania, Hobart, Australia

Abstract
We suggest a new technique for processing GLONASS carrier phase measurements over medium length baselines. This technique exploits the use of IGS products (orbits and clock products) thereby increasing the reliability of ambiguity resolution and reducing the computational burden compared with previous GLONASS processing procedures. To test our proposed new processing technique, we selected three IGS stations in the Australian region and processed both GPS and GLONASS measurements for the period of March 11, 2011. The selected baselines, ranging from 400 – 900 km, gave deviations from 1 cm in the horizontal component and 2 cm in the vertical component between GLONASS and GPS baseline processing and GLONASS results and known IGS ITRF2005 coordinates. This indicates that the proposed technique has promise for continued use. Given improvements in the GLONASS constellation in the coming years, it is likely this technique can be used to process baselines over 1000 km with similar accuracy as GPS.

1. Introduction

The number of GLONASS satellites in orbit has increased gradually since the second-generation satellites, GLONASS-M, were launched in late 2003 and the GLONASS system will reach the complete constellation of 24 satellites this year (October 2011). Positioning applications using GLONASS measurements alone is now becoming a reality. The current GLONASS positioning accuracy can be improved further when we combine GLONASS and GPS observations (Han et al., 1999, Wanninger and Wallstab-Freitag, 2007, Wanninger, 2008 and Stewart et al., 2000). Unlike GPS, GLONASS carrier phase measurements have different frequencies from each satellite in the constellation. This aspect has caused various problems in processing, especially in eliminating common biases in the measurements as well as for achieving ambiguity resolution. The above problems are more serious when processing medium length or longer baselines. Because of ionospheric effects, ambiguities cannot be resolved directly using the L1 or L2 phase measurements. Ambiguity resolution strategies usually rely on using the L3, L5 and L6 (or Melbourne-Wubbena (MW)) combinations (Kleusberg and Teunissen, 1996 and Leick, 2004). For GLONASS, these combinations also suffer from the same frequency problems. Hence, the GLONASS processing procedure includes many complicated steps to gradually eliminate inter-channel biases or receiver clock biases (Habrich, 1999 and Han et al., 1999). Due to the small number of GLONASS satellites in the past, previous researchers usually focused on integrated processing of mixed GPS/GLONASS observations (Habrich, 1999, Han et al., 1999, Wanninger and Wallstab-Freitag, 2007, Wanninger, 2011 and Stewart, 2000). This paper presents a new approach to processing GLONASS carrier phase measurements alone for medium length baselines by using IGS products. This technique gives an improved way of reducing common biases and increasing the success of achieving ambiguity resolution. It also reduces the number of computational steps required to reach an acceptable positioning accuracy. We demonstrate the effectiveness of our technique by processing some medium length baselines in the IGS network. We do not consider baselines longer than 1000 km because the present number of GLONASS satellites observed on such long baselines is below 5 and hence not sufficient for precise processing.

2. GLONASS Carrier Phase Combinations and Processing Procedure

GLONASS carrier phase measurements for dual frequency measurements from receiver i to satellite k can be expressed by the following equations (Habrich, 1999, Kleusberg and Teunissen, 1996 and Leick, 2004).

$$\phi_{i,1}^{k}(t)=\frac{\rho_i^k(t)}{\lambda_1^k}+f_1^k\left[dt_i(t)-dT^k(t)\right]-\frac{I_{i,1}^k(t)}{\lambda_1^k}+\frac{T_i^k(t)}{\lambda_1^k}+N_{i,1}^k+\phi_{i,1}(t_0)-\phi_1^k(t_0)+\varepsilon_{i,1}^k(t)$$

Equation 1

$$\phi_{i,2}^{k}(t)=\frac{\rho_i^k(t)}{\lambda_2^k}+f_2^k\left[dt_i(t)-dT^k(t)\right]-\frac{I_{i,2}^k(t)}{\lambda_2^k}+\frac{T_i^k(t)}{\lambda_2^k}+N_{i,2}^k+\phi_{i,2}(t_0)-\phi_2^k(t_0)+\varepsilon_{i,2}^k(t)$$

Equation 2

Where:

- $\rho_i^k(t)$ is the geometric range from receiver i to satellite k at time t
- f_1^k and λ_1^k are the frequency and wavelength of the L1 carrier phase of satellite k
- f_2^k and λ_2^k are the frequency and wavelength of the L2 carrier phase of satellite k
- $dt_i(t)$ and $dT^k(t)$ are the receiver i and satellite k clock errors at time t
- $I_{i,1}^k(t)$ is the ionospheric delay of the L1 frequency on satellite k at time t
- $I_{i,2}^k(t)$ is the ionospheric delay of the L2 frequency on satellite k at time t
- $T_i^k(t)$ is the tropospheric delay on satellite k at time t
- $N_{i,1}^k$ is the ambiguity parameter of the L1 frequency at time t
- $N_{i,2}^k$ is the ambiguity parameter of the L2 frequency at time t
- $\phi_{i,1}(t_0)$ and $\phi_1^k(t_0)$ are the initial phases of receiver i and satellite k respectively on L1
- $\phi_{i,2}(t_0)$ and $\phi_2^k(t_0)$ are the initial phases of receiver i and satellite k respectively on L2
- $\varepsilon_{i,1}^k(t)$ includes multipath and other noise sources of the L1 frequency at time t
- $\varepsilon_{i,2}^k(t)$ includes multipath and other noise sources of the L2 frequency at time t

The above equations have units of cycles. In terms of units of length, these equations can be rewritten as:

$$L_{i,1}^k(t)=\lambda_1^k\phi_{i,1}^k(t)=\rho_i^k(t)+c\left[dt_i(t)-dT^k(t)\right]-I_{i,1}^k(t)+T_i^k(t)+\lambda_1^kN_{i,1}^k+\lambda_1^k\left[\phi_{i,1}(t_0)-\phi_1^k(t_0)\right]+e_{i,1}^k(t)$$

Equation 3

$$L_{i,2}^k(t)=\lambda_2^k\phi_{i,2}^k(t)=\rho_i^k(t)+c\left[dt_i(t)-dT^k(t)\right]-I_{i,2}^k(t)+T_i^k(t)+\lambda_2^kN_{i,2}^k+\lambda_2^k\left[\phi_{i,2}(t_0)-\phi_1^k(t_0)\right]+e_{i,2}^k(t)$$

Equation 4

Where:

- c is the speed of light in vacuum
- $e_{i,1}^k(t)$ and $e_{i,2}^k(t)$ include multipath and other noise sources of the L1 and L2 frequency at time t in terms of units of length $e_{i,1}^k(t)=\lambda_1^k\varepsilon_{i,1}^k(t)$, $e_{i,2}^k(t)=\lambda_2^k\varepsilon_{i,2}^k(t)$
- L1 and L2 are GLONASS carrier phase measurements for dual frequency, expressed in units of length

2.1 Free Ionospheric Combination, L3

In order to eliminate ionospheric effects, one usually uses the L3 combination. The L3 linear combination equation, in units of cycles, can be derived, using equations (1) and (2) above, as:

$$\phi_{i,3}^k(t)=\alpha_1\phi_{i,1}^k(t)-\alpha_2\phi_{i,2}^k=\frac{\rho_i^k(t)}{\lambda_1^k}+f_1^k\left(dt_i(t)-dT^k(t)\right)+\frac{T_i^k(t)}{\lambda_1^k}+\alpha_1N_{i,1}^k-\alpha_2N_{i,2}^k$$
$$+\alpha_1\left[\phi_{i,1}(t_0)-\phi_1^k(t_0)\right]-\alpha_2\left[\phi_{i,2}(t_0)-\phi_2^k(t_0)\right]+\varepsilon_{i,3}^k(t)$$

Equation 5

Where: $\alpha_1 = \frac{(f_1^k)^2}{(f_1^k)^2 - (f_2^k)^2}$ and $\alpha_2 = \frac{f_1^k f_2^k}{(f_1^k)^2 - (f_2^k)^2}$, $e_{i,3}^k(t)$ includes multipath and other noise sources of the L3 frequency at time t. GLONASS satellites satisfy the frequency relationship $\frac{f_2^k}{f_1^k} = \frac{7}{9}$ (GLONASS, 2002). Therefore the constants $\alpha_1 = \frac{1}{1-49/81} = 2.53125$ and $\alpha_2 = \frac{7/9}{1-49/81} = 1.96875$ do not depend on the satellite frequencies. In terms of units of length, equation 5 can be written as:

$$L_{i,3}^k(t) = \alpha_1 L_{i,1}^k(t) - \alpha_2' L_{i,2}^k(t) = \rho_i^k(t) + c\left(dt_i(t) - dT^k(t)\right) + T_i^k(t) + \alpha_1 \lambda_1^k N_{i,1}^k - \alpha_2' \lambda_2^k N_{i,2}^k + \alpha_1 \lambda_1^k \left[\phi_{i,1}(t_0) - \phi_1^k(t_0)\right] - \alpha_2' \lambda_2^k \left|\phi_{i,2}(t_0) - \phi_2^k(t_0)\right| + e_{i,3}^k(t)$$

Equation 6

where: $\alpha_2' = \frac{(f_2^k)^2}{(f_1^k)^2 - (f_2^k)^2} = \frac{f_2^k}{f_1^k}\alpha_2 = 1.5313$, $e_{i,3}^k(t)$ includes multipath and other noise sources of the L3 frequency at time t in terms of units of length.

2.2 L3 Combinations in Double Differenced Equations.

Equations (5) and (6) still contain clock biases and initial phases. To reduce or eliminate them, one usually forms double differenced equations. Using equation (6), the single differenced observation equation between receivers *i* and *j* to satellite *k* is given by:

$$L_{ij,3}^k(t) = \rho_{ij}^k(t) + c.dt_{ij}(t) + T_{ij}^k(t) + \lambda_1^k\left(\alpha_1 N_{ij,1}^k - \alpha_2 N_{ij,2}^k\right) + \lambda_1^k\left[\alpha_1 \phi_{ij,1}(t_0) - \alpha_2 \phi_{ij,2}(t_0)\right] + e_{ij,3}^k(t)$$

Equation 7

The double differenced observation equation between receivers *i*, *j* and between satellites *k*, *l* is then obtained as:

$$L_{ij,3}^{kl}(t) = \rho_{ij}^{kl}(t) + T_{ij}^{kl}(t) + \lambda_1^l\left(\alpha_1 N_{ij,1}^{kl} - \alpha_2 N_{ij,2}^{kl}\right) + \Delta\lambda_1^{kl} M_{ij,3}^k + e_{ij,3}^{kl}(t)$$

Equation 8

Where:

- $\Delta\lambda_1^{kl} = \lambda_1^l - \lambda_1^k \approx (n_k - n_l)\lambda_1^l \frac{\Delta f_1}{f_1^l}$, and n_k and n_l are channel numbers of satellites *k* and *l* respectively.

  With the present status of the GLONASS constellation, the maximum value of this term is:

  $\left(\Delta\lambda_1^{kl}\right)_{max} \approx (6+7) \times 0.1876m \times \frac{0.5625}{1598.0625} \approx 0.86mm$

  Where:

- $\Delta\lambda_1^{kl} M_{ij,3}^k$ is called the inter-channel bias (IBS), where $M_{ij,3}^k = N_{ij,3}^k + \phi_{ij,3}(t_0)$, $N_{ij,3}^k = \alpha_1 N_{ij,1}^k - \alpha_2 N_{ij,2}^k$, and $\phi_{ij,3}(t_0) = \alpha_1 \phi_{ij,1}(t_0) - \alpha_2 \phi_{ij,2}(t_0)$.
- $\left(\alpha_1 N_{ij,1}^{kl} - \alpha_2 N_{ij,2}^{kl}\right)$ can be rewritten as $\alpha_1 N_{ij,1}^{kl} - \alpha_2 N_{ij,2}^{kl} = \alpha N_{ij,1}^{kl} - \alpha_2 N_{ij,5}^{kl}$,

  Where: $\alpha = \alpha_1 - \alpha_2 = \frac{f_1}{f_1 + f_2} = \frac{1}{1 + 7/9} = 0.5625$

$N_{ij,5}^{kl} = N_{ij,2}^{kl} - N_{ij,1}^{kl}$ is called the widelane ambiguity and can be solved in advance by using the L5 or Melbourne-Wubbena (MW or L6) combinations (Habrich, 1999). When only one ambiguity term remains in equation (8), $N_{ij,1}^{kl}$ is called the narrowlane ambiguity term. The advantage of using equation (8) is that clock biases are completely eliminated. However, the IBS is still present and

potentially affects the ambiguity resolution and accuracy of observations (Habrich, 1999). In fact, Wanninger (2011) points out that the IBS varies considerably depending on the type of receiver used, making carrier-phase ambiguity fixing a complex task. One usually carries out an additional computational step to estimate the IBS by using equation (7), and then eliminate it from equation (8). The IBS residual will not affect the resolution of the ambiguity terms, if we can determine $M^k_{ij,3}$ with an accuracy better than $\frac{\lambda_1^l}{\Delta\lambda_1^{kl}} \alpha \times 0.15\text{cycles} \approx 18\text{cycles}$. If we want to have the IBS residual as small as 1 mm, so that it has a negligible effect in equation (8), $M^k_{ij,3}$ must be determined with an accuracy of better than 1/0.86 ~ 1 cycle. It is very hard to achieve this accuracy because equation (7) still contains receiver clock biases. In order to precisely determine and then eliminate the IBS, Habrich (1999) suggested a complicated procedure that includes seven steps for L1 and L2 processing. If we use the L3 linear combination approach, there are two additional steps for widelane ambiguity resolution. Our technique starts with the use of the L3 observable from equation (5). Using equation (5), we can write the double differenced observation between receivers *i*, *j* and between satellites *k*, *l* as

$$\phi^{kl}_{ij,3}(t) = \frac{\rho^k_{ij}(t)}{\lambda^k_1} - \frac{\rho^l_{ij}(t)}{\lambda^l_1} + \left(f^k_1 - f^l_1\right)\Delta t_{ij}(t) + \frac{\tau^k_{ij}(t)}{\lambda^k_1} - \frac{\tau^l_{ij}(t)}{\lambda^l_1} + \alpha_1 N^{kl}_{ij,1} - \alpha_2 N^{kl}_{ij,2} + \varepsilon^{kl}_{ij,3}(t)$$

Equation 9

In equation (9), we can see that the IBS term is absent, however receiver clock biases still exist. Additionally the frequency term $f^k_1 - f^l_1 = (n_k - n_l)\Delta f_1$ has the largest value of (6+7)*0.5625 = 7.5125 MHz. To obtain sufficient N1 resolution, we need to resolve dt with an accuracy of better than $\frac{0.15\text{cycles} \times \alpha}{f^k_1 - f^l_1} \approx 11$ nsec.

However, to keep the residual of this term within 1mm, dt_{ij} must be determined with an error of less than ~ 0.7 nsec. Han et al., (1999) suggested that the first processing step for combined GPS/GLONASS carrier phase-based positioning was to estimate the receiver clock by using the single differenced pseudo-range observation as:

$$P^k_{ij,3}(t) - \rho^k_{ij}(t) - \tau^k_{ij}(t) = c.dt_{ij}(t) + E^k_{i,3}(t)$$

Equation 10

Where P_3 in equation (10) is computed from P1 and P2 similarly as equation (6), and E_3 includes multipath and other noise sources of the P3 at time t. We will consider the feasibility of this approach. Suppose that errors of the components in equation (10) are distributed as listed in Table 1 when using GLONASS satellite coordinates taken from broadcast ephemerides and IGS ephemerides. In Table 1, the random noise of the GLONASS P-code is assumed to be double that of the GPS P-code (0.3m) because the GLONASS chip lengths of the P-code are twice as long as chip lengths of the GPS code (Wanninger and Wallstab-Freitag, 2007).

Table 1: Errors of various components in a GLONASS pseudo-range measurement

Components in pseudorange	Error magnitude	
	Broadcast ephemeris	IGS ephemeris
E term [6]	0.6 m	0.6 m
ρ	7.0 m	0.2 m
T	0.1 m	0.1 m
dt for 1 measurement	23 nsec	2.1 nsec
dt for 1 epoch	12 nsec	1.1 nsec

If using the broadcast ephemeris and with at least 5 satellites observed at the time of measurement, the receiver clock dt will be determined with an accuracy of $23/\sqrt{4}$=12 nsec. This accuracy of dt should be sufficient for ambiguity (N1) resolution but it may cause an error of ~3cm in equation (9).

2.3 Our Processing Technique

At present, the IGS supplies precise satellite ephemerides for both GPS and GLONASS. According to http://igscb.jpl.nasa.gov/, the accuracy of the GLONASS satellite coordinates in IGS ephemerides is at the 5 cm level. Therefore if the geometric range (ρ) is computed with an accuracy of 0.2 m, we can obtain an estimate of the receiver clock dt with an accuracy of 2.1 nsec. If for each epoch, the receiver can track at least 5 satellites, the accuracy of dt will be $2.1/\sqrt{4}$ = 1.1 nsec, leading to a maximum value of the clock residual in equation (9) being 7.5125 MHz × 1.1 nsec = 0.008 cycles ~ 1.5 mm. Similarly, with only 4 visible satellites, we would have a clock residual error of 0.009 cycles ~ 1.7 mm. If we accept the above errors as being representative of standard IGS products, the procedure of processing GLONASS for medium baselines can be as follows:

- Step 1: Process baselines by using GPS carrier phase measurements.
- Step 2: Estimate receiver clock biases using equation (10) with IGS GLONASS ephemerides and receiver coordinates obtained

from step 1, and then eliminate this bias from equation (9).

- Step 3: Resolve widelane ambiguities N_5 using L5 or L6 (MW), and then exclude them from equation (9)
- Step 4: Resolve narrowlane ambiguities N_1 using equation (9) and then exclude them from equation (9).
- Step 5: Process equation (9) for the last time to compute the baseline components.

The above procedure needs to be performed only once without repetition. Hence the computational burden can be significantly reduced. Also, due to the high accuracy of the receiver clock bias determination, its effect on the observation equation (9) in step 4 is very small (0.008 cycles). This leads to increased reliability of the narrowlane ambiguity resolution.

3. Experiments in Processing GLONASS Baselines using the IGS GLONASS Network

To consider the effectiveness of our processing technique, we used data from three IGS stations in Australia, namely HOB2, MOBS and STR1, for the day of 11 March 2011. These stations are separated by about 450 - 850 km (see Figure 1) and their coordinates are known with high accuracy in ITRF2005 (see Table 2). Figure 2 shows that the number of GPS satellites observed from one of the three possible baselines varies from 6 to 12, whereas the number of GLONASS satellites available is only between 2 – 8.

Figure 1: GLONASS network

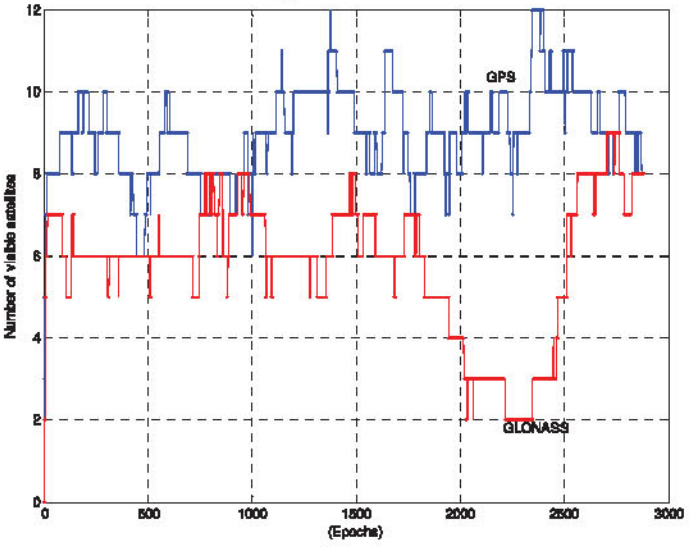

Figure 2: Satellite visibility on baseline STR1-HOBS

Table 2: Coordinates of selected IGS stations in ITRF2005

Site	X (m)	Y (m)	Z (m)	Latitude (deg.)	Longitude (deg.)	Height (m)
	ITRF2005			WGS84		
HOB2	-3950071.9224 +/- 0.0066	2522415.3026 +/- 0.0056	-4311637.7829 +/- 0.0068	-42.80470964 +/- 0.0035	147.43873547 +/- 0.0048	41.0659 +/- 0.0092
MOBS	-4130636.4225 +/- 0.0047	2894953.1083 +/- 0.0040	-3890530.6497 +/- 0.0044	-37.82940768 +/- 0.0025	144.97533923 +/- 0.0033	40.5925 +/- 0.0064
STR1	-4467102.8873 +/- 0.0062	2683039.4809 +/- 0.0052	-3666949.1645 +/- 0.0051	-35.31553028 +/- 0.0027	149.01005371 +/- 0.0045	799.9455 +/- 0.0080

Table 3: Successful rate of GPS ambiguity resolution

Ambiguities	Baselines		
	MOBS-STR1	HOB2-MOBS	STR1-HOB2
N_5	96%	83%	97%
N_1	100%	99%	100%

Table 4: GPS solutions for baselines

Baselines	GPS Baseline vectors (m)		
	ΔX	ΔY	ΔZ
MOBS-STR1	-336466.4614	-211913.6272	223581.4937
HOB2-MOBS	-180564.5034	372537.8074	421107.1151
STR1-HOB2	517030.9525	-160624.1785	-644688.6173

Table 5: Deviations of baseline components from the given IGS values (Table 2)

Baselines	Deviations (m)		
	ΔX/North	ΔY/East	ΔZ/Up
MOBS-STR1	0.000/+0.005	0.000/-0.002	+0.008/-0.007
HOB2-MOBS	-0.003/-0.012	+0.002/ 0.000	-0.018/+0.014
STR1-HOB2	-0.009/+0.008	0.000/+0.007	+0.003/+0.001

The averaged number of available satellites for the three baselines is 9 for GPS and 6 for GLONASS. This may make the GLONASS position solutions less accurate than the GPS one and cause some problems for GLONASS ambiguity resolution. Now following the proposed steps of our new processing technique:

Step 1: Baselines are processed first by using GPS double differenced L3 observables, with the successful rates of ambiguity resolution of all baselines listed in Table 3. In the solutions, the widelane ambiguities were solved for by using the MW combination. The final GPS baseline components are listed in Table 4. Table 3 shows that the successful rate of GPS ambiguity resolution is relatively high. As a result, the maximum deviations of GPS baseline components from the known IGS values (Table 2) are 12 mm in the horizontal and 14 mm in the vertical component (see Table 5).

Step 2: Using the GPS solution obtained in step 1 along with the IGS ephemerides, we calculate GLONASS receiver clock biases for each baseline and for each epoch. As a check, we compare the computed GLONASS clock biases with the precise IGS values. Figure 3 shows the comparison available for baseline STR1-HOB2. We can see from Figure 3 that the deviations of the clock errors have a mean value of 0.8 nsec and an RMS value of 0.9 nsec. These values are very close to the estimated value of 1.1 nsec that we made in Table 1, and hence satisfies our requirements.

Steps 3 and 4: Table 6 provides the success rates of GLONASS widelane ambiguity resolution when using the MW and L5 combinations. Compared with GPS, these rates are much lower because the number of GLONASS satellites is smaller and the quality of the GLONASS P-code is also worse. Ambiguities N5 estimated from MW can have an error of ±2 cycles. This potentially causes unfixed or wrongly fixed ambiguities. To overcome this problem, we replace the MW combination with the use of the L5 combination that is already corrected for ionospheric delay using IGS TEC maps. Figure 4 illustrates three cases of estimating the ambiguity N5 by using the MW and L5 combinations and corrected L5 observables.

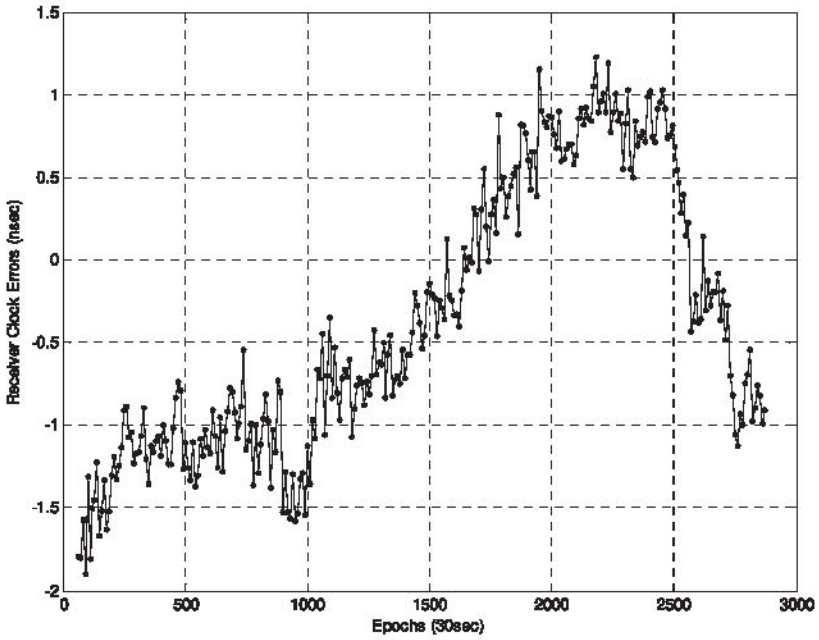

Figure 3: Receiver Clock Errors of baseline STR1-HOB2

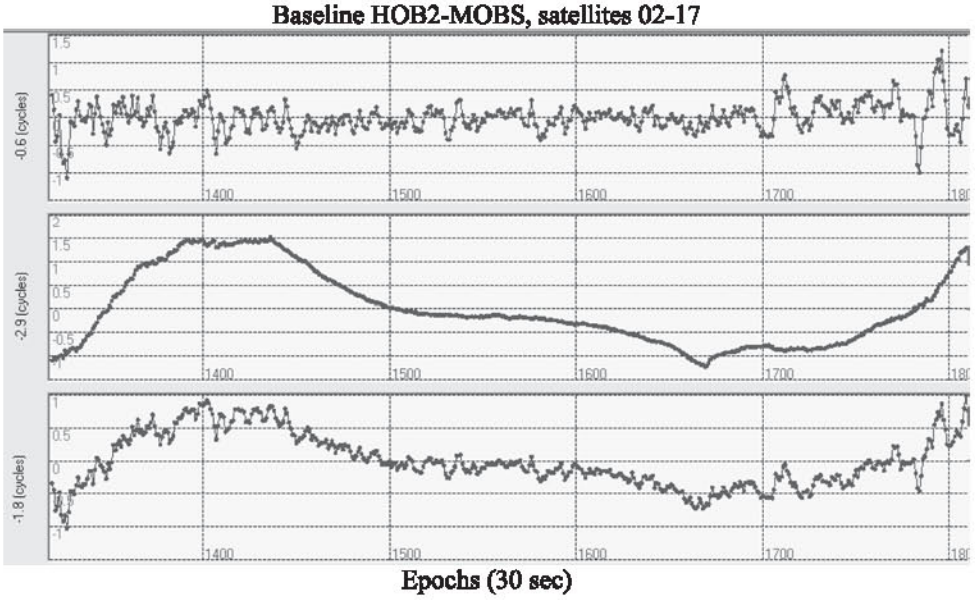

Figure 4: Ambiguity N5 by using MW (top panel), L5 (middle panel) and the corrected L5 combinations (bottom panel)

The corrections computed from IGS TEC maps mainly represent general variations of ionospheric effects. The corrected L5 combinations still contain short period ionospheric effects, which may cause some problems in widelane ambiguity resolution.

To take into account these effects, we estimate one ionospheric zenith delay parameter per 3 hours. The last two rows of Table 6 show considerable improvements of widelane ambiguity resolution using L5 compared with using MW.

Table 6: Successful rate of GLONASS widelane ambiguity resolution

Ambiguities	Baselines		
	MOBS-STR1	HOB2-MOBS	STR1-HOB2
N_5 using MW	96%	56%	61%
N_5 using L5	93%	73%	78%
N_1	100%	93%	91%

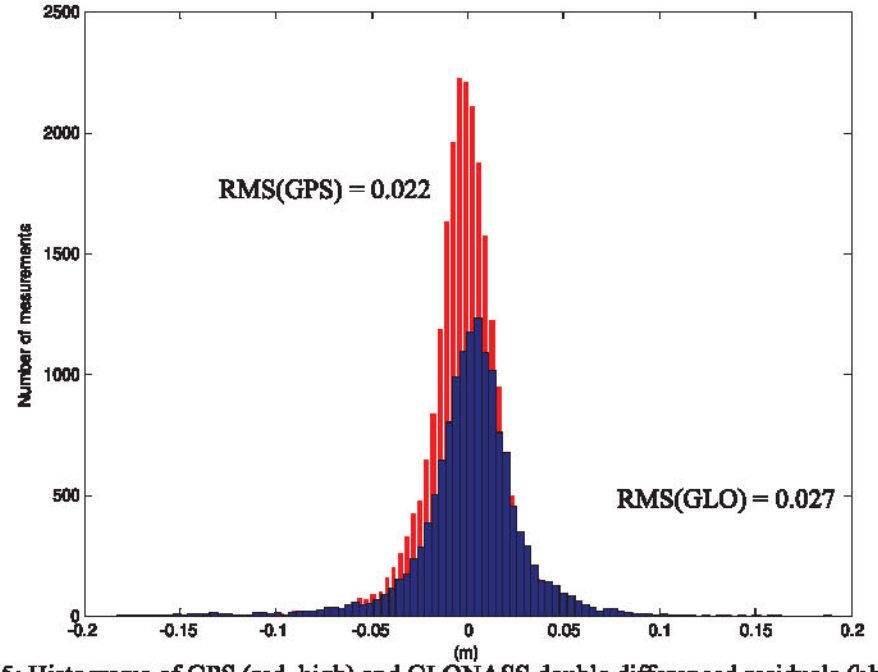

Figure 5: Histograms of GPS (red, high) and GLONASS double differenced residuals (blue, low)

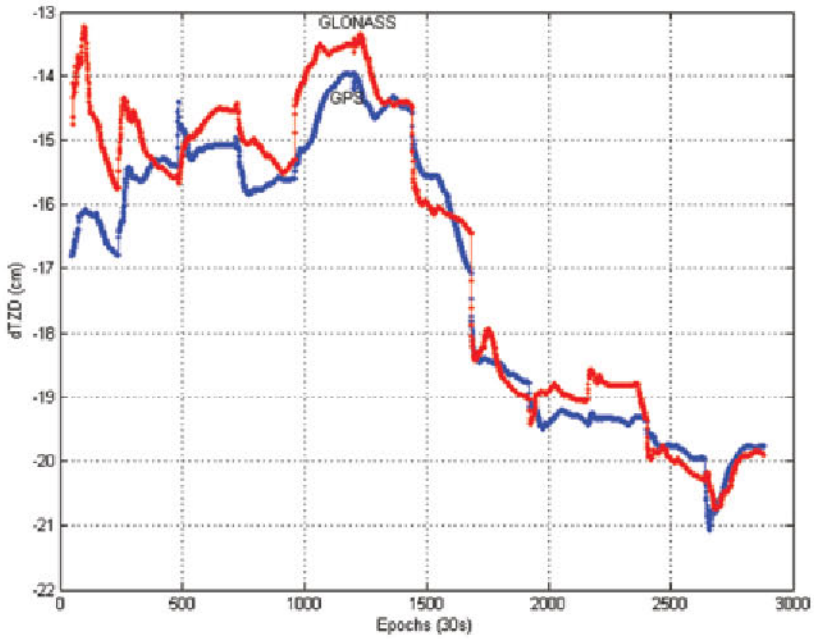

Figure 6: Tropospheric zenith delay on baseline MOBS-STR1

Table 7: GLONASS solutions for baselines

Baselines	GLONASS Baseline vectors (m)		
	ΔX	ΔY	ΔZ
MOBS-STR1	-336466.4636	-211913.6347	223581.4994
HOB2-MOBS	-180564.4968	372537.8022	421107.1348
STR1-HOB2	517030.9550	-160624.1666	-644688.6277

Table 8: Deviations of baseline components from the given IGS values

Baselines	Deviations (m)		
	ΔX/North	ΔY/East	ΔZ/Up
MOBS-STR1	-0.002/+0.008	-0.007/+0.005	+0.014/-0.012
HOB2-MOBS	+0.003/-0.001	-0.004/+0.001	+0.002/-0.005
STR1-HOB2	-0.006/+0.003	+0.012/-0.004	-0.009/+0.017

Table 9: Deviations of baseline components between GLONASS and GPS

Baselines	Deviations (m)		
	ΔX/North	ΔY/East	ΔZ/Up
MOBS-STR1	-0.002/+0.003	-0.007/+0.007	+0.006/-0.005
HOB2-MOBS	+0.006/+0.011	-0.006/+0.001	+0.020/-0.019
STR1-HOB2	+0.003/-0.005	+0.012/-0.011	-0.012/+0.016

Step 5: After correcting N5 and N1 ambiguities from equation (9), we process equation (9) for the last time with the unknowns being the three baseline components and tropospheric zenith delay (TZD) parameters. We model the TZD parameter as a random walk process with one parameter per 2 hours. Figure 5 shows histograms of the corresponding GPS and GLONASS L3 double differenced residuals. They have RMS values of 22 mm and 27 mm respectively. Figure 6 shows the values of TZD estimated from GPS and GLONASS measurements for baseline MOBS-STR1. The maximum deviation of TZD values between GPS and GLONASS is about 1cm. Finally we compare the GLONASS solution with the known IGS values and the computed GPS solution. The results are given in Tables 7-9. The above results show that the agreement between our GLONASS solution and the known IGS values, and between the GLONASS and GPS baseline solutions are approximately 1 cm in horizontal and 2 cm in vertical components, despite some specific GLONASS disadvantages. Whilst we have only given a limited baseline comparison using a single day of observations in this paper, we believe that these results are representative of what can be achieved with our new technique. This is confirmed by our more extensive processing not reported here (the deviations above are statistically zero–ie., GPS and GLONASS are equal).

4. Discussion

To reduce the effects of ionospheric delay on medium length baselines, ambiguity resolution is usually based on using the L3 linear combinations. However, due to different frequencies between GLONASS satellites, these combinations still contain some biases, such as inter-channel biases (IBS) or receiver clock biases. L3 combinations (using equation (8) in units of length) have the advantage of being without receiver clock biases but they still consist of IBS, whereas L3 combinations in terms of units of cycles (equation (9)) do not have IBS but do have receiver clock biases. Procedures for processing equations (8), (9) or both are complicated and have to be used repeatedly to gradually eliminate the various bias terms. We suggest a new processing technique based on using IGS products. This procedure is only carried out once therefore it greatly reduces the computational burden. Additionally the technique has the advantage of increasing reliability of ambiguity resolution for medium length baselines. Despite some disadvantages of the GLONASS system, such as the insufficient number of satellites and low quality P-code, our processed results show that the accuracy of our GLONASS solutions can be achieved at 1 cm in the horizontal and 2 cm in the vertical components. This is the same as the accuracies obtained by our GPS solutions.

With the improvement of the GLONASS constellation over the coming years, it is likely that similar results can be achieved over baselines greater than 1000 km.

Acknowledgements
This paper is part of the results of a project carried out by the Vietnam Institute Geodesy and Cartography.

References

GLONASS, 2002, "Interface Control Document Version 5.0", Coordinate Scientific Information Center.

Habrich, H., 1999, "Geodetic Application of the Global Navigation Satellite System (GLONASS) and of GLONASS/GPS Combination", University of Bern, 51.

Han, S., Dai, L., and Rizos, C., 1999, "A New Data Processing Strategy for Combined GPS/GLONASS Carrier Phase-Based Positioning", *12th Int. Tech. Meeting of the Satellite Division of the U.S. Inst. of Navigation*, Nashville, Tennessee, 14-17 September,1619-1627.

Kleusberg, A., and Teunissen, P. J. G., 1996, "GPS for Geodesy", Springer-Verlag, Berlin.

Leick, A., 2004, "GPS Satellite Surveying", John Wiley and Sons, Canada.

Stewart, M. P., Tsakiri, M., Wang, J., and Monico, J. F., 2000, "The Contribution of GLONASS Measurements to Regional and Continental Scale Geodetic Monitoring Regimes", *Journal of Earth, Planets, Space*, 52, 877-880.

Wanninger, L., and Wallstab-Freitag, S, 2007, "Combined Processing of GPS, GLONASS, and SBAS Code Phase and Carrier Phase Measurements, Proceedings of ION GNSS 2007, 866-875.

Wanninger, L., 2008, "The Future Is Now: GPS+GLONASS+SBAS = GNSS", GPS World, July 2008, 42-48.

Wanninger, L., 2011, "Carrier-Phase Inter-Frequency Biases of GLONASS receivers", *Journal of Geodesy*, Published online: 02 August 2011.